Development of an Analysis Method for Power Cable Creepage Phenomenon in the Duct

Koki Kashiro[*1], *Katsumi Iwamura*[*1], *Tomonori Kamibayashi*[*2], *Tadanori Nagayama*[*2], *Hiroyasu Nishikubo*[*3]

ABSTRACT In a duct system, which is an underground cable laying system, a phenomenon called cable creepage phenomenon may occur in which the cable in the duct moves in the traveling direction of the vehicle. If this phenomenon progresses excessively, there is a concern that serious damage may occur in the vicinity of the cable joint. It is necessary to accurately grasp the moving force of the cable to solve for the phenomenon. However, in the past, studies using empirical formulas were mainly adopted, and there was a discrepancy with the actual result.

For this reason, in this research, we focused on the horizontal displacement of the duct when a vehicle passes through it, and developed a new theory using the behavior of the displacement difference between the cable and the duct at that time. In addition, an analysis system for the creepage using the theory was developed. In order to confirm the validity of the theory, we conducted a full-scale experiment and compared the experimental values with the theoretical values to reconcile the two.

1. INTRODUCTION

Underground cables in Japan are often installed inside ducts, and in this installation system, it is feared that a phenomenon called creepage phenomenon occurs, in which the cables inside ducts move in the direction of travel of a vehicle, as shown in Figure 1. The phenomenon tends to occur in soft ground, shallow duct depths, and heavy traffic conditions. The phenomenon is regarded as a problem because, when it occurs, the longitudinal shape of the cable in the manhole changes, and the stress of the cable concentrates near the joint, causing serious damage.

Since the method of restraining the cable in the manhole is the main mitigation against the phenomenon, it is necessary to accurately grasp the moving force generated in the cable. However, conventional calculations of the movement forces generally follow formulas based on experiments[1)], and the problem is that they differ from the actual situation.

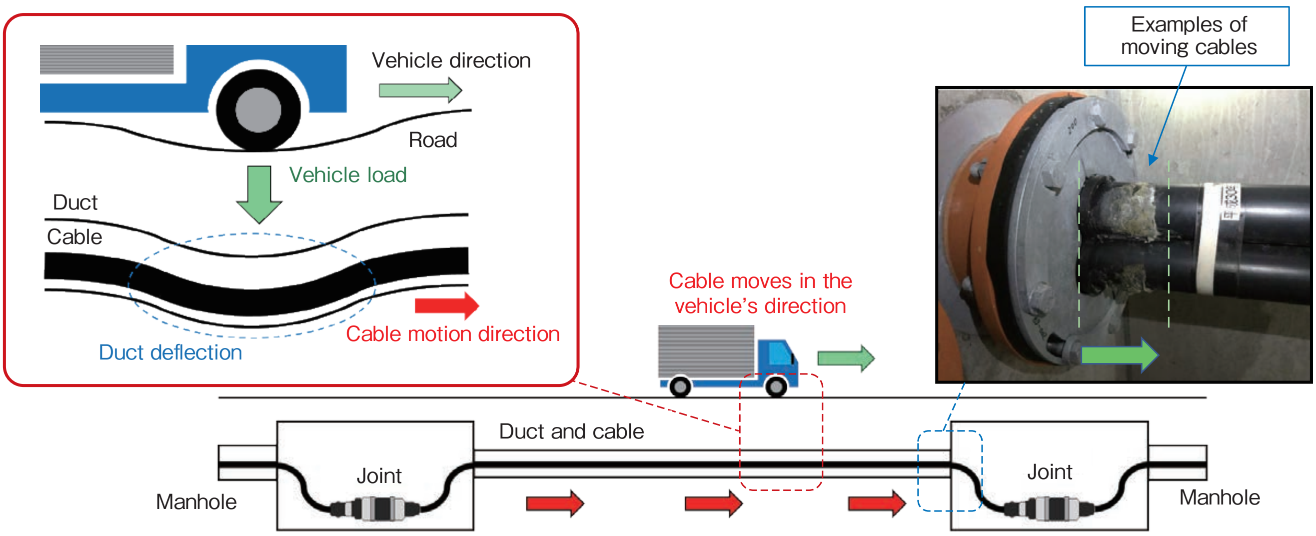

Figure 1 Schematic diagram of the cable creepage behavior.

*1 Power Cable Engineering Department, Cable System Installation Section, FURUKAWA ELECTRIC CO.,LTD
*2 Transmission Line & Substation Construction Center, TOHOKU ELECTRIC POWER NETWORK CO.,INC
*3 CAE System Department, Business Solution Division, FITEC Corporation

Previously reported studies predominate the theory that the vertical component of the duct defection plays an important role.

According to the surf-riding theory proposed by Timmis in 1937[2], it was reported that “a cable experiences unequal vertical deflection in the duct before and after the wheels of a passing vehicle, and the length of contact with the cable is longer at the rear. This creates a horizontal component of thrust that pushes the cable forward, like a surf-rider gliding along a surf edge.” However, this report did not explain the reason for the unequal deflection of the duct, and reported that the calculated elongation of the cable based on the surf-riding theory was much smaller than the measured value[3].

In addition, in a paper by Kim et al. in 1999[4], it was reported that “the local longitudinal (horizontal) velocity of the duct changes when a vehicle passes through the forward area (positive direction) and backward area (negative direction) appears, and the cable generates a frictional force in the longitudinal direction with the duct. On the other hand, the vertical sinking amount of the duct due to the vehicle load is greater in the backward area than in the forward area. Therefore, the lateral elasticity of the cable reduces the contact pressure between the duct and the cable in the backward area. As a result, the static friction force between the two in the backward area is reduced, causing a slip, and the cable moves forward.” However, as for the contact pressure between the duct and the cable in the negative area which is explained in the Kim’s paper[4], we tried the Finite Element Analysis Method (FEAM) for the contact pressure under the condition of the Japanese equipment, the result was that it did not decrease significantly. Therefore, the authors discovered that the decrease in contact pressure due to the deflection of the vertical component of the duct is not the main cause of the cable creepage phenomenon in the Japanese plant.

For the above reasons, the authors developed a new theory that explains the mechanism by which the vehicle caused the creepage in the cable using the Amonton-Coulomb’s friction law. The Amonton-Coulomb’s friction law[5] is an empirical rule where the kinetic friction force does not depend on the sliding velocity. In other words, similar to Kim et al., the source of the driving force for the movement of the cable is considered to be the forward speed area and backyard speed area in the local longitudinal direction of the duct generated by the passage of the vehicle, and the Amonton-Coulomb’s friction law was applied on these two areas. As a result, the magnitude of the dynamic friction force acting on the cable becomes the same, and the acting length is longer in the forward movement area than in the backward movement area. For this reason, the amount of friction force acting in the forward direction is greater than that in the backward direction, and the movement of the cable becomes conspicuous.

In this report, we describe a newly developed theory, the development of a creepage analysis system which can be easily analyzing the cable movement force and its amount using a normal PC, the verification of the validity of the theory by a full-scale experiment[6], and the tendency of occurrence of creepage phenomenon using the analysis system.

2. DEVELOPMENT OF A NEW THEORY OF THE CREEPAGE PHENOMENON

The kinetic friction force is the driving force of the creepage phenomenon, the mechanism of generating the kinetic friction force is assumed as follows.

(1) When the load of the vehicle is applied to the road in which the duct is buried, the duct bends and the displacement occurs in the horizontal direction.
(2) The movement of the vehicle causes a velocity in the horizontal displacement of the duct.
(3) The cable elastically deforms as the duct is displaced.
(4) Since the displacement of the cable cannot follow the displacement of the duct, a displacement difference occurs between the two, and this displacement difference moves as the vehicle moves.
(5) Due to the movement of this displacement difference, a sliding velocity is generated under the condition of this displacement difference between the cable and the duct.
(6) Based on the Amonton-Coulomb’s friction law, the generation of the above sliding velocity results in a constant dynamic frictional force.

Each step is explained in detail in this chapter.

2.1 Displacement Analysis of Ground (Duct)

Using the FEAM software (general-purpose nonlinear structural analysis solver), we analyzed the displacement of the ground when a vehicle load was applied on the ground surface. The analysis conditions used are the same as those for the full-scale experiments described in Chapter 4. Figure 2 shows the analysis conditions. The ground was composed of three layers, and each layer was treated as an elastic body with different Young’s modulus and Poisson’s ratio. In Figure 2, the duct is illustrated at a depth of 1.2 m, but the duct is not modeled on the assumption that it will be displaced together with the ground in the FEAM analysis. The vehicle load is a concentrated load of 20 tf, and the 1.2 m above the duct is moving in the longitudinal direction from -4.8 m (load position A) to 4.8 m (load position E), and the ground displacement analysis point was set directly under the load C. The figure below shows the FEAM results of the ground displacement at the analysis points in the figure. As the vehicle position changes from A->B->C->D->E, the ground at the analysis point is displaced vertically and longitudinally. The maximum longitudinal displacement was 16 μm, and the maximum vertical displacement was 90 μm. The amount of displacement inside the elastic body when a concentrated load is applied to the surface of a homogeneous semi-infinite elastic body can be calculated by the Boussinesq's formula[7], and it has been confirmed that this formula approximately reconcile with the result of FEAM analysis.

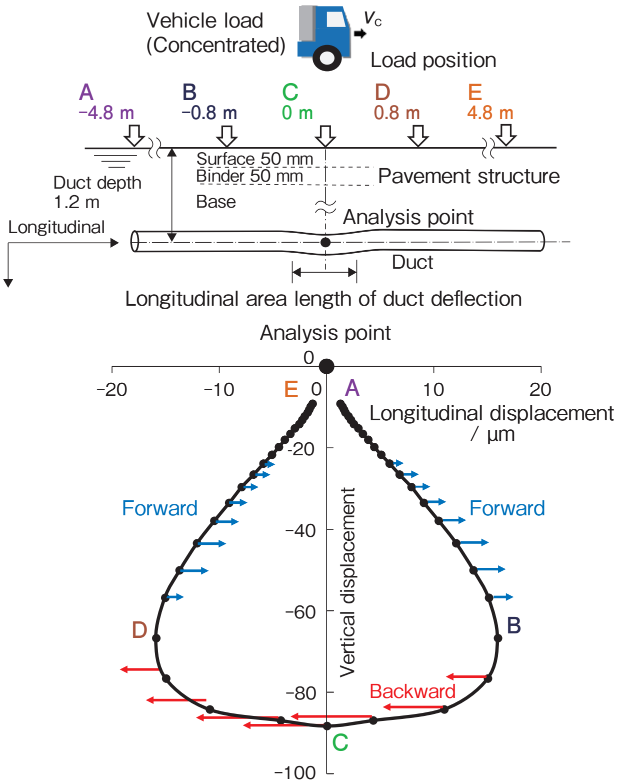

Figure 2 Analysis conditions for the ground displacement and the ground displacement for each vehicle load position (FEAM).

Figures 3 and 4 are graphs of the vertical component and horizontal (longitudinal) component of the ground displacement shown in Figure 2. In these figures, the horizontal axis indicates the position in the longitudinal direction of the duct, and the traveling direction of the vehicle is the increasing direction of the x-axis, and the vehicle load is acting on the origin point (load position C in Figure 2). In addition, Figure 5 shows a schematic diagram of the state of deflection of the duct on the occurrence. As indicated by the vector shown in Figure 5, the duct is deflected by the load of the vehicle, and is displaced in the horizontal direction of the duct. The vertical component of the displacement shown in Figure 3 is buckling about the load position and the longitudinal component of the displacement shown in Figure 4 as it extends radially. The amount of deflection becomes steep in the vicinity of the load position, and the effect of the vehicle load decreases as the distance from the load position increases, and the amount of deflection gradually decreases.

2.2 Longitudinal Velocity of Ground (Duct) Displacement

When the vehicle moves in the x direction with velocity v_c, the ground deflection moves with the same velocity. If the longitudinal displacement distribution of the ground (duct) displacement in Figure 4 is represented by $D_l(x)$, the propagation in the x-axis direction at time t is represented by $D_l(x\text{-}v_c t)$. By differentiating this with respect to time, V_l is obtained and expressed by the formula (1).

$$V_l(x - v_c t) = \frac{\partial D_l(x - v_c t)}{\partial t} = -v_c \frac{\partial D_l(x - v_c t)}{\partial x} \qquad (1)$$

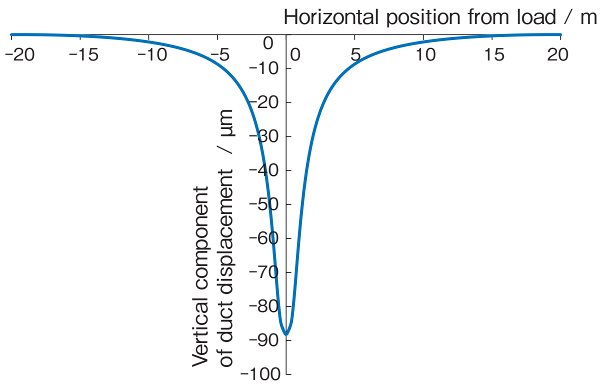

Figure 3 Longitudinal distribution of the vertical component of ground (duct).

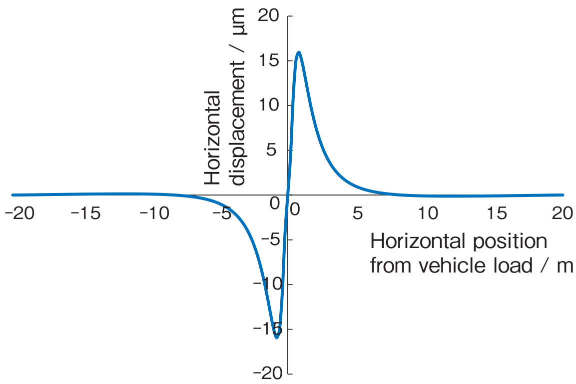

Figure 4 Longitudinal distribution of the longitudinal component of ground (duct) displacement.

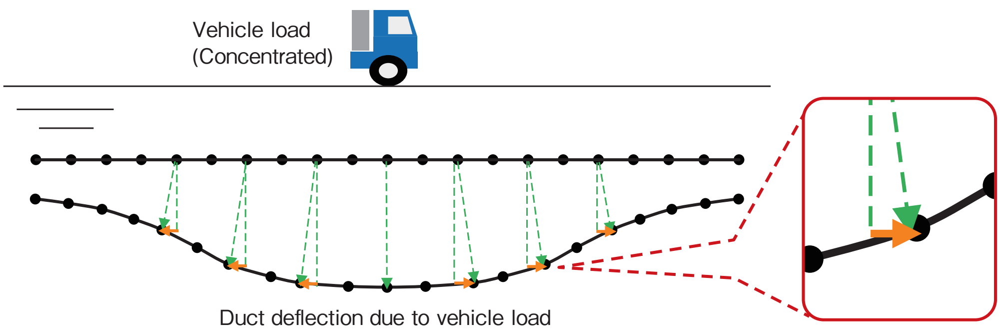

Figure 5 Longitudinal component distribution of ground (duct) displacement caused by vehicle.

Figure 6 shows the x-axis distribution of V_l calculated from equation (1) when the vehicle passes the load position C (x = 0) at a speed v_c=40 km/hr. Areas in the forward direction (the same direction as the vehicle moves) near x = 0 and the peripheral backward direction (the opposite direction as the vehicle moves) appear in V_l. Comparing these two areas, the magnitude of the velocity is large in the backward direction area near x = 0 where the change in displacement is steep, and the area length is long in the forward direction area where the displacement amount gradually decreases. The product of the velocity magnitude and the area length will be the same as shown in Figure 6, and the longitudinal displacement of the duct will return to its original position once the vehicle has passed.

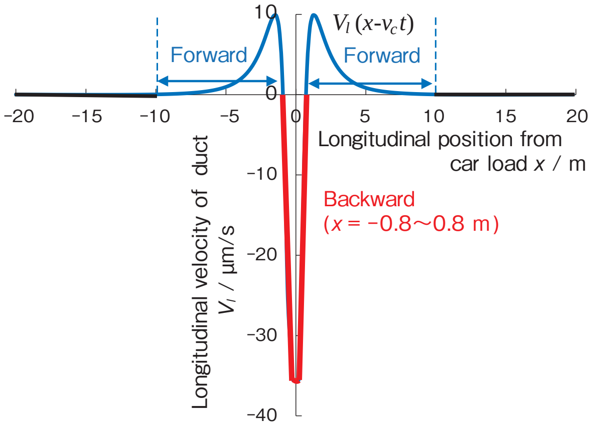

Figure 6 Longitudinal distribution of longitudinal velocity V_l of the ground (duct).

2.3 A New Theory on the Occurrence Mechanism of the Creepage Phenomenon

With the movement of the duct in Figure 6, the cable is elastically displaced by static friction and follows. If the elastic displacement amount is smaller than the duct displacement amount, a displacement difference occurs between the two. When the displacement difference progresses at the speed of the vehicle, a sliding speed occurs between them. The sliding velocity consists of a forward direction that is the same as the direction of travel of the vehicle and reverse direction that is opposite to the vehicle. Based on the Amonton-Coulomb's friction law, which states that the magnitude of the dynamic friction does not depend on the sliding speed, as shown in Figure 7, the dynamic friction is applied at a constant value according to the change in the forward and back ward directions. Comparing the two areas, the absolute value of the dynamic friction forces is the same, but the area length is larger in the forward direction. The product of the magnitude of the kinetic friction force and the length of the area is greater in forward motion than in backward motion. The above discussion summarizes the relationship shown below and we consider the creepage phenomenon based on the relationship in this theory.

The absolute value of the maximum dynamic friction forces:
(forward) = (backward)
The length of the area of the dynamic friction forces:
(forward) > (backward)
(the absolute value) × (the length of the area):
(forward) – (backward) > 0

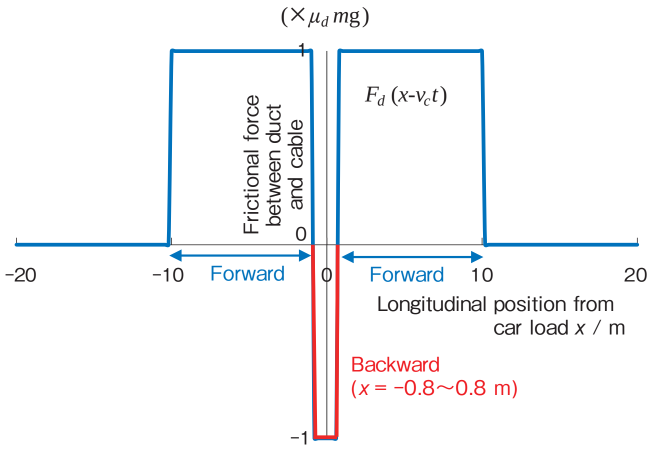

Figure 7 Longitudinal distribution of dynamic friction force between duct and cable.

Also, the effects of the static frictional force and the dynamic frictional force according to the above theory on the cable is explained with reference to Figure 8. Along with the horizontal displacement of the duct, the static frictional force acts on the cable in the longitudinal direction, and the cable follows along with the duct. Assuming that the amount of displacement in the longitudinal direction of the duct is ΔD, $\Delta D_l - \Delta C_l = 0$ at this time. On the other hand, the displacement difference between the cable and duct is generated when $\Delta D_l - \Delta C_l > 0$.

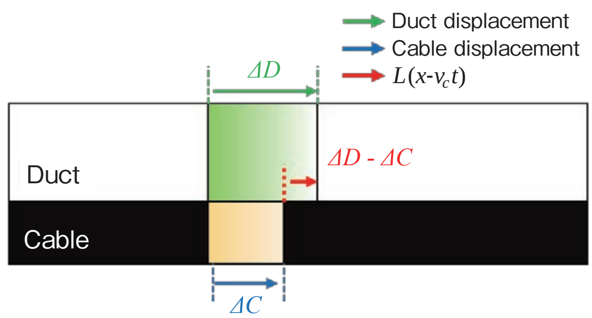

Figure 8 The image of horizontal displacement between cable and duct.

When this displacement difference between the duct and the cable propagates in the x direction at the speed v_c of the vehicle, a dynamic friction force F_d (x-$v_c t$) acts on the cable. The distribution of the dynamic friction force is the same as in Figure 8, the absolute value is the same and the area length in the forward direction is longer than the backward.

Therefore, when the dynamic frictional force F_d (x-$v_c t$) is propagating to Δx section of the cable, the cable is displaced in the forward direction in the Δx section with respect to the duct. The elastic elongation of the cable generated by the dynamic friction force is retained and accumulated by the static friction force between the duct and the cable.

3. DEVELOPMENT OF A NEW ANALYSIS MODEL FOR THE CREEPAGE PHENOMENON ANALYSIS AND DEVELOPMENT OF AN ANALYSIS SYSTEM

Based on the theory regarding the creepage phenomenon shown in Chapter 2, an analysis model was designed and an analysis system was built in order to obtain the movement force.

3.1 A New Analysis Model for the Creepage Phenomenon

Since the longitudinal displacement and velocity of the duct shown in Figures 4 and 6 are local to the entire length of the cable, the cable is divided into a constant length Δx, and modeled as a joint lattice of mass m and longitudinal elastic modulus k for this analysis, as shown in Figure 9.

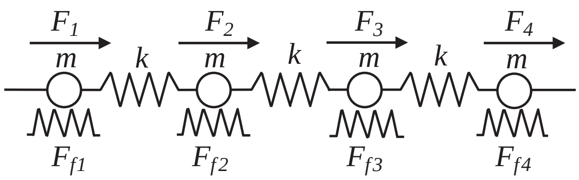

$$F_f = -\left(\frac{2}{1+e^{b(V_l \Delta t - u(t))}} - 1\right)\mu_d mg \qquad (2)$$

m : Mass of cable element (mass point),
F_f : Kinetic frictional force acting on mass point (N),
g : Gravitational acceleration (m/s),
μ_d : Dynamic friction coefficient, Δt : Minute time interval (s),
V_l : Relative velocity between mass point and duct (m/s),
$u(t)$: Displacement of mass point between Δt (m), b : Shape factor

Figure 9 Discrete element model for the cable creepage analysis.

For each discrete length Δx of the cable, the magnitude of the dynamic friction force F_f is calculated from Equation (2) as a constant value that does not depend on the sliding speed, and given to each mass point. Equation (2) is a differentiable sigmoid function, which enables the stabilization of numerical calculations. The shape factor b is a constant that takes into account the shear deformation of the cable sheath[8], and by using this sigmoid function, the behavior considering the shear deformation of the cable sheath due to the occurrence of displacement between the cable and the duct, shown in Figure 10, is reflected.

A dynamic friction force F_f is given to each mass point of the cable shown in Figure 9. From the equilibrium condition of the cable elastic force and the inertial force in Equation (3), the creepage force (the internal stress of cable) F and the displacement U of the mass point (the elastic stretch of cable) are calculated. By repeating this calculation every minute time, the creepage force is calculated.

$$[k]\,\vec{U} + [m]\,\vec{a} = \vec{F} + \vec{F_f} \qquad (3)$$

$\vec{F}$: The creepage force vector of cable (the internal stress of cable) (N),
$\vec{U}$: Mass point displacement vector (the elastic stretch of cable) (m),
$\vec{a}$: Mass point acceleration vector (m/s^2),
$[k]$: Stiffness matrix ($k=EA/\Delta L$), $[m]$: Cable mass matrix (N),
$\vec{F_f}$: Dynamic friction force vector on mass point (N)

As described above, the newly developed theory was reflected in the analysis system.

3.2 Development of the Creepage Force Analysis System

In order to facilitate the cable design and maintenance, we have developed a creepage analysis system that runs on a PC with normal specifications. Ground displacement was analyzed by axisymmetric element FEAM in a cylindrical coordinate system with the central axis perpendicular to the road. By approximation that the vehicle is a concentrated load and the duct is displaced together with the ground, the analysis is reduced to two dimensions that do not change of the circumferential direction of the cylindrical coordinate system, and the calculation time is greatly reduced. The ground is treated as an elastic body, and five layers with different elastic properties can be set so that the standard road structure in Japan can be approximated. The cable analysis was performed with a longitudinal one-dimensional discrete element method, as shown in Figure 9. Boundary conditions at the ends of the cables are constrained or released, and in order to study mitigations against the creepage phenomenon, constraining conditions by springs are made possible.

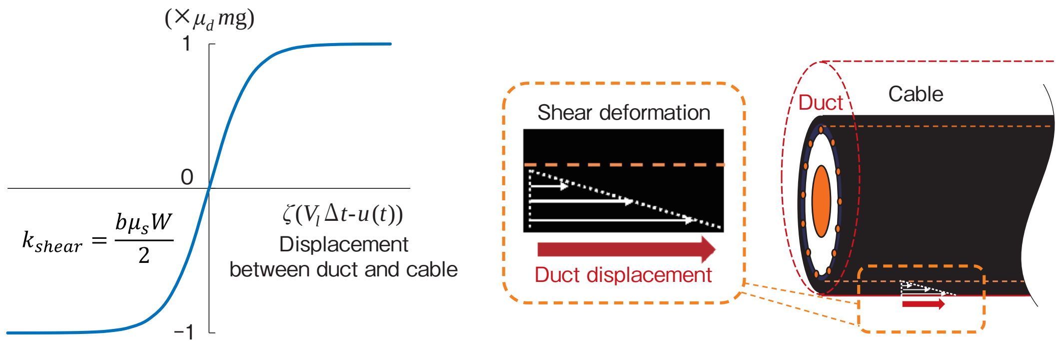

Figure 10 Shape factor *b* using a sigmoidal function.

4. FULL-SCALE EXPERIMENTS ON THE CREEPAGE PHENOMENON

4.1 Overview of Full-scale Experiments

For the purpose of verifying the validity of the new theory about the creepage phenomenon, a full-scale experiment was carried out, and the creepage phenomenon force, the analytical value, and the experimental value were compared. The experimental conditions are shown in Figure 11 and Table 1. The length of the cable (duct) is 30 m, which is about 1/10 of the actual equipment. A PFP (Polyester Concrete Fiberglass Reinforced Plastic Pipe) was used for the duct. Two ducts were laid at a depth of 1.2 m. A single-core cable was laid in one duct with three strands per hole. In the other duct, six acceleration sensors were installed at intervals of 1 m to measure acceleration in the vertical direction of the duct. In this report, we concluded that the creepage phenomenon is caused by the longitudinal displacement of the duct, but we also measured the vertical displacement of the duct in this experiment. This is because the amount of displacement in the vertical direction of the duct is six times as large as the amount of displacement in the longitudinal direction, so the amount of displacement can be measured with a high accuracy. The ground surface was simply paved, and a 20 ton truck was repeatedly run in one direction at speeds of 20, 30, and 40 km/h. The cable end (upstream end) on the entry side of the truck was left open. At the exit cable end (downstream end) of the track, a load cell was used to measure the compressive force of each cable. The vertical deflection of the duct was calculated to be 90 to140 μm from the measured acceleration. The deflectional length of the longitudinal area of the duct was 7 to 11 m. The width of these measurements is independent of track speed and is an empirical variation.

4.2 Comparison of the Experimental Results and the Analytical Values of the Creepage Phenomenon

Figure 12 is a comparison of the experimental results and the analytical results under the experimental conditions. Circle and square plots are experimental values, and solid and dashed lines are analytical values. The values for the cables on the lower phase side and the upper phase side are shown, respectively. In the analysis conditions, the weight of the two lower phase cables was set to be 1.5 times assuming that the weight of the upper phase cable is evenly applied to the two lower phase cables. The coefficient of dynamic friction between the duct and the cable was μ_d = 0.27. The dynamic friction force acting on the upper phase cable with the lower phase cable sheath was set to μ_d = 0.25 smaller than the dynamic friction force with the duct. The analytical values agreed well with the experimental values, confirming the validity of the theory developed in this study. The creepage force tends to saturate at about 900 N for the lower phase cable and about 550 N for the upper phase cable. Such saturation characteristics of the cable creepage force have been reported in the actual measurement results[3].

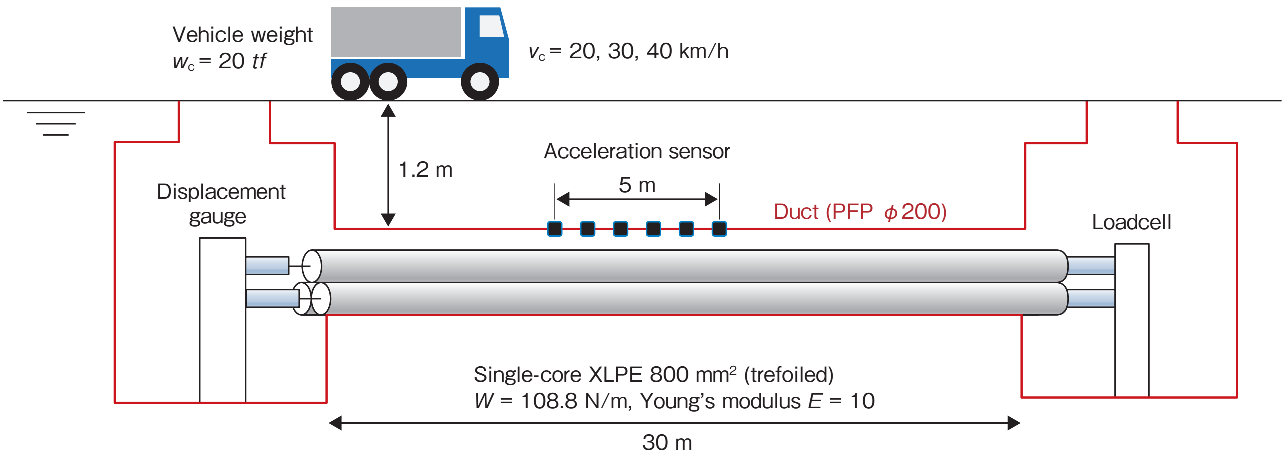

Figure 11 Overview of the full-scale experiment.

Table 1 The full-scale experiment conditions for the cable creepage.

Item	Experimental conditions			
Cable	Single core cable XLPE 800mm^2 (W = 108.8 N/m, Young's modulus E = 10), Three strands per unit			
Duct	PFP ϕ 200, Depth d = 1.2 m, Cable (duct) length L = 30 m			
Vehicle	Vehicle weight W_c = 20 tf, Vehicle speed V_c = 20, 30, 40 km/h			
Road	Pavement layer	Thickness mm	Young's modulus MPa	Poisson's ratio
	Surface	50	4,000	0.35
	Binder	50	800	0.35
	Roadbed/subgrade	Deeper than 100 mm	800	0.4
Duct deflection (Measured values)	Vertical displacement: 90 - 140 μm Longitudinal area length of the deflection: 7 - 11 m			

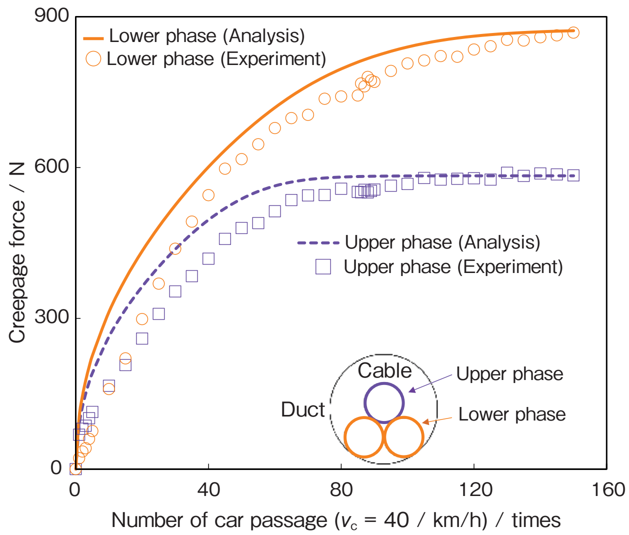

Figure 12 Experimentally and analytically obtained values of the creepage force.

5. INVESTIGATION OF OCCURRENCE TENDENCY OF CREEPAGE PHENOMENON USING THE ANALYSIS SYSTEM

It has been reported that soft ground and shallow burial depth of ducts are conditions that facilitate the creepage phenomenon. In addition, single-core cables tend to be more susceptible to the creepage than triplex cables. In this chapter, under the general facility conditions in Japan, the creepage phenomenon was analyzed for each condition, and the occurrence conditions were investigated.

5.1 Creepage Phenomenon Analysis Study Conditions

In order to clarify the occurrence tendency of the creepage phenomenon, the following conditions were selected as analysis conditions that mainly affect the elastic deformation of the cable.

(1) Cable type (single core cable, triplex cable)
(2) Action range of frictional force acting on the cable duct

The above will be explained in detail.

In this theory, it is assumed that the occurrence condition of the dynamic friction force, which is the driving force, is generated by the difference in longitudinal displacement between the cable and the duct, and it is presumed that the easiness of elastic deformation of the cable affects the creepage phenomenon.

As for the type of cable, the modulus of longitudinal elasticity is different between the single-core cable and the triplex cable, and the triplex cable is more likely to be displaced.

Also, the acting length of the frictional force acting on the cable duct affects the elastic displacement of the cable as shown in Figure 13. As shown in Figure 13, the elastic displacement ΔC of the cable is inversely proportional to the longitudinal elasticity EA of the cable, and proportional to the square of the acting length X of the static friction force μ acting on the cable. For this reason, it was inferred that the acting length affects the generation of the displacement difference between the cable and the duct.

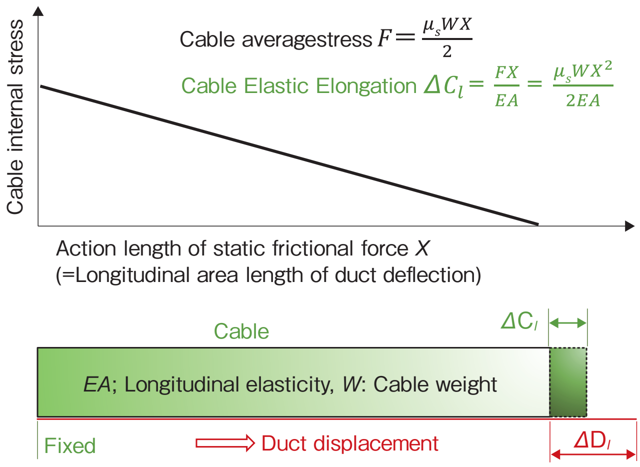

Figure 13 Elastic displacement of the cable when the friction force is applied.

Based on the above, the conditions were selected as shown in Tables 2 and 3. In order to grasp the tendency, Table 2 was used as the condition of the type of cable and the coefficient of dynamic friction.

Regarding Table 3, it is the condition of the duct and

Table 2 Cable condition for the cable creepage analysis.

Items \ Cable		Single-core (XLPE 800 mm^2)	Triplex (XLPE150 mm^2)
Mass W	N/m	108.8	112.7
Longitudinal elasticity $EA \times 10^6$	N	8.01 (Young's modulus E = 10)	1.47 (E = 3.3)
Dynamic Friction coefficient μ_d		0.3, 0.4, 0.5	0.3, 0.4

Table 3 Cable and vehicle conditions for the cable creepage analysis.

Item		Set value		
Duct burial depth d	m	0.6	1.5	2
Vehicle weight W_c	tf	8.57	20	27.17
Longitudinal displacement of duct	μm	35.7		
Duct length L	m	300		

the vehicle. A duct length of 300 m is a general facility condition for actual facilities in Japan. The speed of vehicle was v_c = 40 km/h.

Regarding the cable burial depth, it is generally known that the deeper the cable burial depth, the more difficult for creepage to occur, The main purpose is to affect the acting length of the frictional force (the above (2)) by increasing the weight of the vehicle according to the depth. Specifically, by setting the maximum displacement in the longitudinal direction of the duct at each depth at a constant 35.7 μm, the analysis implies that the deeper the duct, the greater the weight of the vehicle. This creates a condition in which the duct is deeper and the vehicle is heavier, therefore the length of the frictional force of the cable increases.

5.2 Analysis Results and Trend of the Creepage Phenomenon Generation Conditions

The Figure 14 shows the change in creepage force with respect to the number of vehicle passages under the analysis conditions shown in the Tables 2 and 3.

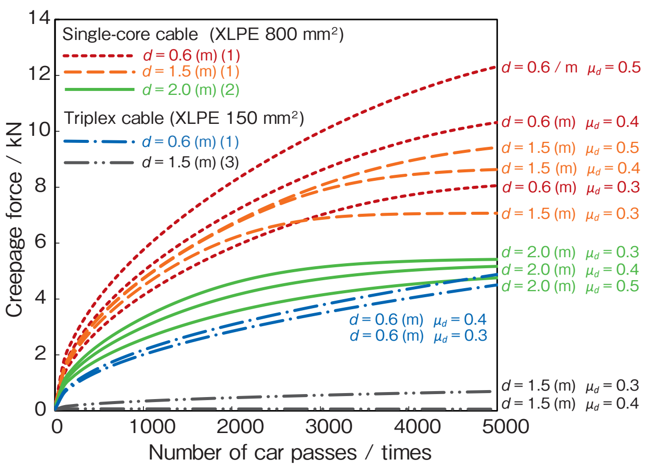

Figure 14 Variation of the maximum cable force with the number of vehicle passages.

When comparing the results of the creepage force for each type of cable based on this analysis, on one hand the single-core cable with a large longitudinal elasticity had a large creepage force. On the other hand, the creepage force of the triplex cable was much smaller than that of the single-core cable. As for the triplex cable with a low longitudinal elasticity, it is inferred that the cable follows the displacement of the duct.

In addition, depending on the condition of the burial depth of the duct (the acting length of the frictional force), the increase and decrease tendency of the creepage force accompanying the increase of the frictional force differed. On one hand when the buried depth of the duct was shallow (when the acting length of the frictional force was short), the creepage force increases due to the increase in the frictional force. On the other hand, when the duct was buried deep (when the acting length of the frictional force was long), the creepage force decreased due to the increase in the frictional force.

It has been reported that the change in the buried depth of the duct makes it more susceptible to direct impact from vehicles. In addition, to the above, this analysis also revealed that the burial depth of the duct affects the relationship between the frictional force and the creepage force.

Based on the above results, from the relationship between the elastic displacement amount ΔC_l of the cable and the longitudinal displacement amount ΔD_l of the duct, the conditions for generating the cable creepage force can be classified as shown in Table 4 below.

Table 4 Occurrence conditions of the cable creepage.

	Equipment conditions	Creepage force	Length of ΔC_l and ΔD_l
(1)	Single core cable d = 0.6 m, 1.5 m	Increment: μ_d large	Both of forward and backward area: $\Delta C_l < \Delta D_l$
(2)	Single core cable d = 2.0 m	Decline: μ_d large	forward area: $\Delta C_l \fallingdotseq \Delta D_l$ backward area: $\Delta C_l < \Delta D_l$
(3)	Triplex cable d = 1.5 m	Almost zero at μ_d = 0.4	Both of forward and backward area: $\Delta C_l \fallingdotseq \Delta D_l$

d: duct depth, μ_d: dynamic friction coefficient

Depending on the conditions, it was found that the increasing and decreasing tendency of the magnitude of the creepage changed with the increase and decrease of the dynamic friction force μ_d, and that the cable with a low elastic modulus (Young's modulus) tended to generate less creepage force.

6. CONCLUSION

The authors reported that the creepage phenomenon is caused by the local longitudinal displacement of the duct caused by the load of the vehicle. This occurs due to the following mechanisms.

(1) Vehicle loads cause local deflections in underground ducts. This deflection has a longitudinal displacement component. Due to this longitudinal displacement of the duct, a static frictional force acts on the cable, and the cable is elastically displaced. When the amount of elastic displacement of the cable is smaller than the amount of displacement in the longitudinal direction of the duct, a displacement difference occurs between the two.

(2) As the vehicle moves longitudinally on the duct, the displacement difference between them also moves at the same vehicle speed, producing local longitudinal velocities in the duct and cable. The local longitudinal velocity of the duct consists of a forward direction area in the direction of travel of the vehicle and a backward direction area in the opposite direction.

(3) Based on the Amonton-Coulomb's friction law, which states that the dynamic friction force does not depend on the sliding speed, the dynamic friction

force is treated as a constant value that does not depend on the sliding speed. When the friction law is applied to the relative velocity of the duct and cable in the longitudinal direction, the amount of dynamic friction acting on the cable is greater in the forward direction than in the backward direction as follows. The difference in the amount of action of this dynamic friction force causes the cable to move forward.

The absolute value of the maximum dynamic friction forces:

(forward) = (backward)

The length of the area of the dynamic friction forces:

(forward) > (backward)

(the absolute value) × (the length of the area):

(forward) – (backward) > 0

Based on this theory, we have developed a creepage phenomenon analysis system that can be easily used on an ordinary PC for cable design and maintenance. Furthermore, we verified the validity of the theory by conducting a full-scale experiment and confirming that the measured values and the analytical values are in good agreement. By using the developed cable creepage analysis system, it became possible to examine the occurrence tendency of the creepage phenomenon.

REFERENCES

1) Electric Technology Research Association: "The present and future engineering technology applied for XLPE cables installation (in Japanese)", 61 (2005).
2) A.C. Timmis: "The Creepage of Underground Cable", POEEJ, 30 (1937), 180.
3) Y. Watanabe, K. Kanazawa, T. Sasaki: "MEASURES AGAINST CREEPAGE OF 275KV HPFF CABLE", IEEE Transaction on Power Delivery, 4 (1989), 25.
4) J.K. Kim, J.S. Yi: "Kinematics of Cable Creepage" IEEE Transactions on Power Delivery, 14 (1999), 1.
5) Valentin L. Popov: "Contact Mechanics and Friction" Springer, (2010).
6) T. Kamibayashi, Tadanori Nagayama, Nobumitsu Tamai, Junpei Nakai, Masahiko Murata, Hiroyasu Nishikubo: "Development of Analytical Method for Cable Creepage Phenomenon in Duct (in Japanese)" IEEJ Transactions on Power and Energy, 140 (2020), 277.
7) K.L. Johnson: "Contact mechanics", Cambridge University Press, (2008).
8) T. Kamibayashi, Manabu Sakata, Hiroyuki Ebinuma, Toshikazu Yamamoto, Masahiko Murata, Hiroyasu Nishikubo: "A Study of the Power Cable Creepage in the Duct (No.6) (in Japanese)" 2018 National Convention Record, IEE Japan, 127 (2018), 198.